tvst

Article

Biofeedback Rehabilitation and Visual Cortex Response in Stargardt's Disease: A Randomized Controlled Trial

Paolo Melillo[1,*], Anna Prinster[2,*], Valentina Di Iorio[1], Gaia Olivo[3], Francesco Maria D'Alterio[1], Sirio Cocozza[3], Mario Quarantelli[2], Francesco Testa[1], Arturo Brunetti[3,*], and Francesca Simonelli[1,*]

[1] Eye Clinic, Multidisciplinary Department of Medical, Surgical and Dental Sciences, University of Campania Luigi Vanvitelli, Naples, Italy
[2] Institute of Biostructure and Bioimaging, National Research Council, Naples, Italy
[3] Department of Advanced Biomedical Sciences, University of Naples Federico II, Naples, Italy

Correspondence: Francesco Testa, Eye Clinic, Multidisciplinary Department of Medical, Surgical and Dental Sciences, University of Campania Luigi Vanvitelli, Via S. Pansini, 5, 80131 Naples, Italy. e-mail: francesco.testa@unicampania.it

Received: September 11, 2019
Accepted: March 12, 2020
Published: May 11, 2020

Keywords: Stargardt disease; visual rehabilitation; biofeedback; visual cortex

Citation: Melillo P, Prinster A, Di Iorio V, Olivo G, D'Alterio FM, Cocozza S, Quarantelli M, Testa F, Brunetti A, Simonelli F. Biofeedback rehabilitation and visual cortex response in Stargardt's disease: a randomized controlled trial. Trans Vis Sci Tech. 2020;9(6):6, https://doi.org/10.1167/tvst.9.6.6

Purpose: to evaluate the effect of biofeedback (BF) rehabilitation on the visual function and on the activity of primary visual cortex (PVC) in patients with Stargardt's disease owing to mutations in the *ABCA4* gene (STGD1).

Methods: This was a single-center, controlled, randomized study. Twenty-four patients with STGD1 were randomized into two groups: a treatment group (TG) undergoing BF rehabilitation and a control group (CG). Treatment with BF consisted of a 10-minute session per eye performed weekly for 12 weeks. The subjects underwent a baseline and 3-month follow-up visits, including best-corrected visual acuity (BCVA), reading test, microperimetry, and functional magnetic resonance imaging (fMRI). The fMRI studies were acquired sequentially using a passive viewing condition and an active reading task. The primary outcomes were the change in the fMRI activation of primary visual cortex and the change in reading ability.

Results: After treatment, the patients in the TG were able to read smaller characters ($P = 0.002$) with a greater reading speed ($P = 0.014$) compared with patients in the CG. The fMRI studies showed a significant effect ($P < 0.001$) of BF on primary visual cortex activation in the TG compared with the CG. Finally, we observed significant ($P < 0.05$) improvements of best-corrected visual acuity, macular sensitivity, and fixation stability parameters in the TG compared with the CG.

Conclusions: Our study showed that visual rehabilitation using BF improved the usage of residual visual function in patients with STGD1.

Translational Relevance: Our findings show that the BF treatment compared with no treatment at all resulted in benefits. The specificity of the treatment could be examined to determine whether BF can be included in clinical practice.

Introduction

Stargardt's disease, first described in 1909, is the most frequent form (1:8000) of juvenile macular degeneration; the majority of people affected by the disease presents with uncorrectable, decreased visual acuity during their teenage years, which most often progresses to legal blindness.[1] Loss of central vision strongly impairs everyday life activities, such as locomotion, reading, and face recognition. Commonly, the disease is transmitted in an autosomal recessive manner and is related to *ABCA4* gene mutations (STGD1).[2] Visual function in patients with macular degeneration is notoriously difficult to predict; two patients with apparently identical clinical features can exhibit very different levels of impairment. These differences are frequently ascribed to adaptive strategies adopted by patients. One such adaptive strategy is to develop an eccentric retinal spot outside the scotoma, the preferred retinal locus (PRL), as a new fixation point.[3] A PRL can be defined as a discrete retinal area that contains the center of a target image for 20% of a fixation interval.[4]

The consequences of the PRL development on visual perception remain unclear. It has been shown that a sizable proportion of patients use more than one PRL for a given task.[5–8] Furthermore, some patients describe themselves as looking straight ahead when they are fixating with the eccentric PRL; this phenomenon has been referred to as adaptive eccentric fixation or oculomotor re-referencing.[9]

To date, there is no approved effective medical intervention for the disease; where the traditional treatment cannot offer further results, improvement through biofeedback (BF) training in patients who suffer from macular diseases either remaining stable or worsening is of interest and well worthy of attention.[10] BF visual rehabilitation represents a novel effective therapeutic approach for training and stabilizing the PRL; it has been applied in different ocular pathologies characterized by visual deterioration and loss of fixation stability.[10,11] The reasons for this improvement are probably due to the fact that we trained a retinal motor PRL, with appropriate retinal sensitivity, and this training increases the number of correct fixation saccades and re-references the oculomotor system.[10] Andrade et al.[12] have shown that patients are usually unaware of their scotoma because when the retina is damaged by a local lesion (induced scotoma), the cortical neurons driven by stimuli originating in this region do not remain inactive but become selective to stimuli originating in other parts of the retina. Cortical neurons located in the retinotopic position corresponding with the scotoma receive some degree of activity from the unimpaired neurons in the area surrounding the lesion.[12] BF training, with its sound stimulation, increases the conscious attention of the patient,[13,14] thereby facilitating the lock-in of the visual target and increasing the permanence time of the target itself on the retina. This mechanism probably facilitates stimuli transmission between intraretinal neurons as well as between the retina and brain, where the highest degree of stimuli processing takes place, thereby supporting a "remapping phenomenon."[13]

According to the possibility of a "neuroplasticity phenomenon," the purpose of our study was to evaluate the effectiveness of BF rehabilitation by investigating both the modifications of the visual function and the effects on the activity of the primary visual cortex (PVC) in patients with STGD1.

Methods

Patients

This was a single-center, controlled, randomized (1:1) study, conducted, from March 2016 to December 2016, at the Referral Center for Hereditary Retinopathies of the Eye Clinic of the University of Campania "Luigi Vanvitelli" with the collaboration of University of Naples Federico II and the Biostructure and Bioimaging Institute of the National Research Council.

The present study conformed to the tenets of the Declaration of Helsinki and was approved by the local Institutional Review Board of the University of Campania "Luigi Vanvitelli" (formerly named Second University of Naples). Written consent to participate in the study was obtained from all participants.

Eligible participants were subjects who met the following inclusion criteria: clinical and molecular diagnosis of STGD1, age 8 years or older, visual acuity in both eyes of less than 1.3 logarithm of the minumum angle of resolution, and a willingness to participate in the study. Exclusion criteria were participation in a clinical study with an experimental drug or ocular surgery in the last 6 months, pregnancy, foveal sparing, and other concomitant ophthalmologic pathologies (e.g., glaucoma, cataract) that could interfere with the interpretation of the results.

Eligible patients were randomized into two groups: a treatment group (TG; 12 patients) that underwent BF rehabilitation, and a control group (CG, 12 patients) that did not undergo any therapy. Block randomisation (size = 24) was done by a computer-generated random number list prepared by an investigator with no clinical involvement in the trial. The examiner who was responsible for MP1-BF rehabilitation, after obtaining the patient's consent, telephoned a contact person who was independent of the recruitment process for allocation consignment. Whereas the patient and the examiner responsible for MP1-BF rehabilitation were aware of the allocated arm, technicians and physicians performing the other clinical investigations (i.e., ophthalmic examination and MRI) and data analysts (i.e., who check spatial normalization in MRI processing) were kept blinded to the allocation.

For each patient in the TG, an upper area of 2° with highest microperimetry (MP) sensitivity was identified to be rehabilitated. During the treatment, the patients maintained fixation by looking at a red cross placed within the 2° circular area, guided by a sound: the sound became continuous when the patient fixed the correct area and became intermittent when it was lost. In the first session, the examiner instructed the patient on how to move the eye to focus the red cross with the selected area to keep the sound as continuous as possible. During rehabilitation, the other eye was occluded. Treatment with MP1-BF consisted of a 10-minute session per eye performed once a week for 12 consecutive weeks.

Ophthalmologic Examination

At baseline and at the 3-month follow-up visit, all patients underwent fMRI and a complete ophthalmologic examination, which included best-corrected visual acuity (BCVA), reading test, slit-lamp biomicroscopy of the anterior segment and fundus examination, optical coherence tomography (OCT), and MP. A full-field electroretinogram (ERG) was performed only at baseline.

According to research attempting to investigate genotype–phenotype in patients with STGD1,[15] variants of *ABCA4* mutations have been classified as likely null (including stop codon variants, frameshift, and splicing defects), and missense; hence, patient genotypes were classified into three groups: (A) at least two missense variants, (B) at least one missense variant and a likely null variant, and (C) two likely null variants.

BCVA was measured by Early Treatment Diabetic Retinopathy Study criteria and converted into logarithm of the minumum angle of resolution for analysis.

Reading capacity was assessed with Colenbrander test by measuring two parameters: the smallest size of the print character (minimum print size) expressed in M-units that can be read without significant errors; the average reading speed (RS) expressed in words per minute.

Fundus lesions were classified according to Fishman et al.[16] as follows:

- Phenotype I included patients with small atrophic appearing foveal lesions and localized perifoveal yellowish-white flecks;
- Phenotype II included patients with numerous yellowish-white fundus lesions throughout the posterior pole; and
- Phenotype III included patients with extensive atrophic appearing changes in the retinal pigment epithelium (RPE).

OCT was performed with Cirrus HD-OCT (Carl Zeiss, Dublin, CA). The acquisition protocol comprised both a five-line raster scan and a macular cube scan pattern (512 × 128 pixels) in which a 6 × 6-mm region of the retina was scanned within a scan time of 2.4 seconds. The retinal thickness analysis protocol provided with the instrument software was used to calculate the central retinal thickness (CRT); normal value of central retinal thickness was 262 ± 16 µm.[17] Moreover, the sub-RPE slab was obtained for each examination using the commercially available software on the Cirrus HD-OCT (version 6.0). The sub-RPE slab is an en face visualization using only the light penetrating below the RPE into the choroid and sclera; these en face fundus images were then used to measure the area of the RPE lesion RPE-A, expressed in millimeters squared, using a recently developed and validated algorithm.[18] Further details about the automated algorithm and its application in STGD1 can be found elsewhere.[19]

MP was performed by an automatic fundus-related perimeter (MP1 Microperimeter; Nidek Technologies, Padova, Italy). The following parameters were used: a fixation target of 2° in diameter consisting of a red cross and a white, monochromatic background with a luminance of 1.27 cd/m^2. Retinal sensitivity was measured using a 10-2 pattern, covering 10° centered onto PRL with Goldman size III stimuli with intensity ranging from 0 to 20 dB and with a projection time of 200 ms. The following MP parameters were computed: mean sensitivity and dense scotoma size (DSS). The DSS was the diameter, expressed in degrees, of the area in which the stimuli were not seen with the brightest light intensity (0 dB).[20]

Moreover, the fixation stability was assessed both in terms of the percentage of fixation points that fell within a 2° (FS2°) and 4° diameter (FS4°) circle during the MP test and in terms of the bivariate contour ellipse area (BCEA), as previously described.[21] Finally, the eccentricity and polar angle of the PRL were assessed. Eccentricity is the distance between the PRL and the fovea in degrees of visual angle; the polar angle is the angle between the upward vertical axis from the fovea and a line connecting the PRL, and the fovea in a clockwise direction in retinal coordinates.

Full-field ERG was recorded by corneal contact lens electrodes with a Ganzfield stimulator (Reticom; Roland Consult, Brandenburg, Germany) according to the recommendations of the International Society for Clinical Electrophysiology of Vision.[22] ERG abnormalities were classified into three groups based on the following criteria proposed by Lois et al.[23]: group I had normal full-field amplitudes; group II had normal dark-adapted ERG but reduced light-adapted b-wave amplitudes; and group III had ERG abnormalities involving both dark-adapted and light-adapted b-wave amplitudes. The normal ERG amplitude values were between 95 and 305 µV for b-wave in 0.01 dark-adapted response, 90 to 250 µV for b-wave in light-adapted 3.0 response, and 57 to 223 µV for 30-Hz flicker response.

Functional MRI Data Acquisition

Functional MRI data were acquired at 3 Tesla (Trio, Siemens Medical Systems, Erlangen, Germany) using an echoplanar imaging sequence (TR = 3000 ms;

TE = 34 ms; and thirty-eight 3-mm-thick axial slices covered the whole brain; pixel size 1.8 × 1.8 × 3 mm^3) and an eight-channel head radiofrequency coil.

The visual stimulus was designed using Presentation (Neurobehavioral Systems, Berkeley, CA), and administered through MRI compatible googles using a commercially available system (VisualStim Digital, Resonance Technology, Northridge, CA), which allowed the correction of refraction errors and unilateral stimulation.

Functional MRI studies were acquired sequentially using two separate conditions: passive viewing and active reading.

For the passive viewing condition, patients were administered a visual stimulus consisting of a black-and-white square checkerboard, with a constant light intensity of 5 lux, inverting at a frequency of 8 Hz, alternated every 15 seconds with a black background. The contrast between black and white squares is maximal (100%). The checkerboard matrix size was 8 × 6, and the width of each check is 3.75°, so that a viewing angle of 30° × 22.5° is stimulated. For both the activation (checkerboard) and rest (black screen) phases, a white cross was displayed in the central 2° of the field of view, and the patients were instructed to fix their gaze on it.

In total, for each eye 65 time points were acquired, including 5 initial volumes that were discarded from the subsequent analysis, to allow for MR signal stabilization.

For the active reading condition, we designed a fMRI paradigm based on four-letter word recognition task, following the one proposed by Ming et al.[24] The paradigm used a block design consisting of six cycles; each cycle was composed of a rest period of 30 seconds followed by a stimulus period of 30 seconds. It began with 15 seconds of discarded data acquisition (to ensure equilibrium of the longitudinal magnetization). Orthogonal vertical and horizontal guidelines with a width of 0.4° were provided to help patients locate the targets in each paradigm. During the stimulus period, a four-letter word was presented at the center of the screen. Subjects were asked to press one switch if the word represented a living thing and the other switch if the word represented a nonliving thing. The word presented was changed every 3 seconds. Each letter subtended 2°. The rest condition required maintained fixation on a 2° cross that was located at the center of the screen.

For both the passive viewing and active reading conditions, each subject repeated the task twice, one for each eye, first with the right eye and then with the left one.

Functional MRI Data Preprocessing

MRI data were preprocessed using the Statistical Parametric Mapping 8 package (SPM8, the Wellcome Department of Neurology, London U.K.; http://www.fil.ion.ucl.ac.uk/spm).

The following preprocessing steps were performed: correction of between-slice acquisition time shifts by interpolation of the fMRI time series; and rigid body co-registration of each fMRI volume to the first time point of the corresponding fMRI series.[25]

The six head motion parameters derived from the previous frame-wise volume co-registration were entered in subsequent first level analysis along with their first derivatives, to remove signal fluctuations related to motion.

Resulting datasets were then normalized to the standard Montreal Neurological Institute echoplanar imaging template and resampled to a voxel size of 2 × 2 × 2 mm^3.

An experienced operator, blind to the condition of the subject, assessed the accuracy of the spatial normalization.

A high-pass temporal filter (0.008 Hz) was then applied to the normalized echoplanar imaging volumes to remove slow signal drifts with a period longer that 125 seconds.

Finally, before statistical analysis, normalized activation maps were smoothed using a Gaussian kernel of 6 mm full width at half maximum to minimize the impact of interindividual anatomic variability and normalization inaccuracies, and to grant normal distribution of the data as per the Gaussian random field model underlying the statistical process used for adjusting P values.[26]

For each hemisphere, four spherical regions of interest (ROIs) (a 5-mm radius) were defined in the Montreal Neurological Institute space according to Plank et al.,[27] sampling the PVC along the calcarine fissure from the occipitopolar area to its extreme anterior margin. Coordinates (x, y, z) of the ROIs in the Montreal Neurological Institute space were respectively [±6, −100, − 6], [±6, −90, 0]; [±6, −80, 6] and [±6, −70, 10]. According to Wandell et al.,[28] these regions correspond with specific retinotopic areas: PVC1 (the most posterior one) corresponds with the central 5° of the visual field, PVC2 from 5° to 10° of central visual field, PVC3 from 10° to 15°, and PVC4 (the anteriormost ROI) for central visual field beyond 15°.

The ROIs were masked by the activation map resulting from the voxels showing a significant activation ($P < 0.05$ family-wise error (FWE)-corrected at voxel level) over the whole dataset at any of the two scans

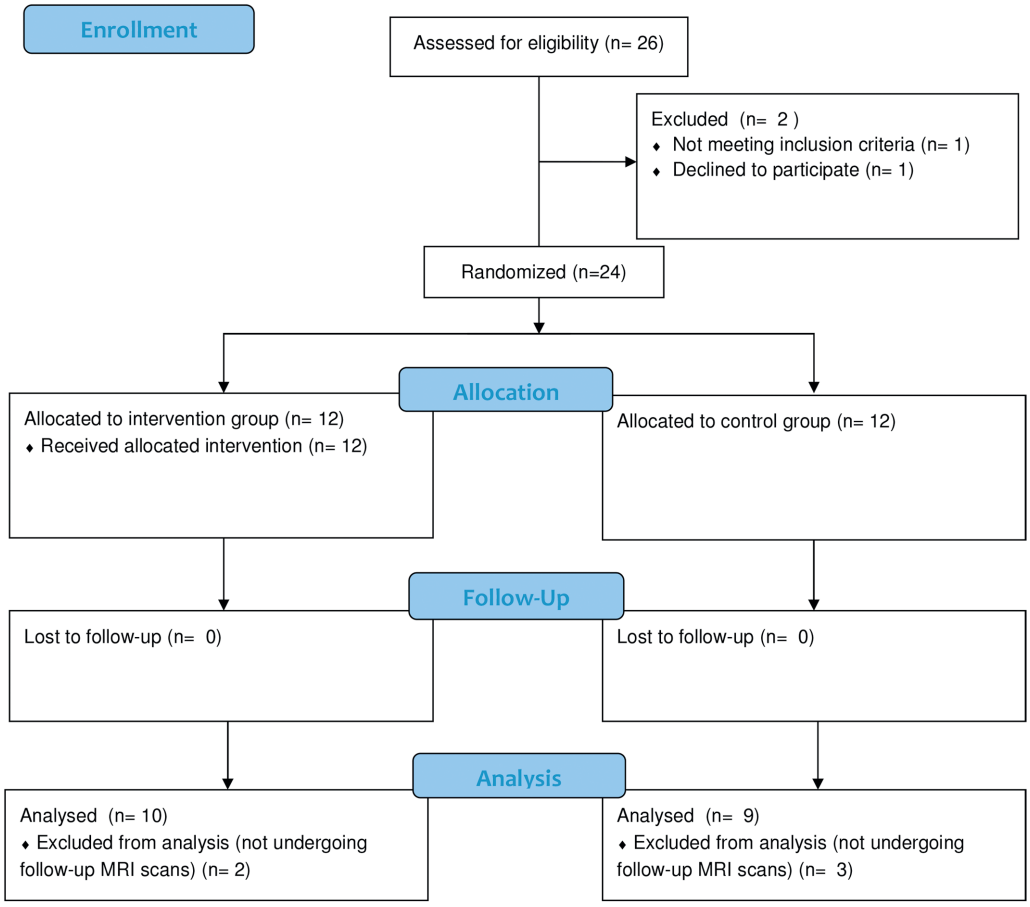

Figure 1. Flow diagram of the study.

(i.e., those showing significant activation when stimulating right and/or left eye) obtained from the checkerboard stimulus data. For each ROI and each subject, the mean t value was extracted and used in subsequent regression analysis.

Statistical Analysis

The primary outcomes were the change in the fMRI activation in the selected ROIs and the change in the RS. The secondary outcomes were the change in BCVA, minimum print size, and MP parameters. The changes were evaluated by fitting repeated-measure longitudinal regression, estimated by a generalized estimating equation. Generalized estimating equations were adopted because this method could deal with the correlated data (e.g., between the 2 eyes/hemispheres of the same person at a given visit, and between values of the same eye followed over time) by adopting an appropriate covariance structure,[29] also in case of non-normality of the data.[30] The value of the beta coefficient (β) is reported together P value and number of independent observation used for its estimations. A P value of less than 0.05 is considered as statistically significant.

Because this was a pilot study, a sample of 24 subjects was chosen following the recommendation of 12 subjects per group, particularly, for feasibility reasons, considering that STGD1 is a rare disease.

Results

Twenty-four patients with a clinical and molecular diagnosis of STGD1 related to mutations of the *ABCA4* gene (16 males and 8 females, mean age 29.2 ± 11.9 years, range 15–54 years) were enrolled and randomized in the two groups.

As shown in Figure 1, all the patients randomized to the TG completed the treatment according to the protocol and all the randomized subjects completed the follow-up examinations according to the protocol, except five patients (three randomized to CG and two randomized to TG) who did not perform the follow-up MRI acquisitions (four refused to undergo an additional MRI and one fMRI was discarded owing to excessive movement during the examination).

Table 1. Demographic, Genetic, and Clinical Data of Patients with STGD1

Patient ID	Sex	Age (years)	Onset (years)	Disease duration (years)	Fundus[a]	ERG[b]	Genotype
TG							
T1	F	19	11	8	II	I	250insCAAA; G1961E; D498N; 4017ins24bp
T2	M	18	14	4	I	I	L541P/A1038V; IVS40+5G->A
T3	M	25	17	8	I	II	L541P/A1038V ; G1961E
T4	F	15	13	2	I	I	G1961E; R2149X
T5	M	48	38	10	III	II	N96D; IVS40+5G>A
T6	M	29	25	4	I	I	G1961E; L1938L; L1894L; S1689P
T7	F	23	14	9	II	III	L541P/A1038V ; F655C
T8	M	33	18	15	I	I	R152Q; G1961E; 402ins24bp
T9	M	21	15	6	I	I	A60V; G1961E
T10	M	25	18	7	II	I	G1961E; R2107H; L949R
T11	M	46	30	16	II	II	N96D; N1436I
T12	M	54	28	26	II	I	N96D; N96D
CG							
C1	M	27	11	16	I	I	G1961E; R2149X
C2	F	51	25	26	II	I	V615A; G1961E
C3	M	21	13	8	II	III	250insCAAA; P402A
C4	F	25	21	4	I	I	R1448K; 5018+2T>C
C5	F	23	18	5	I	I	G1961E; 6282+1G>C
C6	M	49	18	31	III	III	4538insC; IVS40+5G>A
C7	M	20	19	1	I	I	G1961E; R2107H; L949R
C8	M	37	34	3	I	I	G1961E; R2107H; L949R
C9	F	18	10	8	II	II	Y245X; 5714+5G>A
C10	M	19	13	6	I	I	N96D; N96D
C11	M	23	11	12	II	II	G690V; A1598D
C12	F	32	28	4	II	I	G1961E; G1961E

[a]Fundus: (I) a small atrophic-appearing foveal lesion and localized perifoveal yellowish-white flecks; (II) numerous yellowish-white fundus lesions throughout the posterior pole; (III) extensive atrophic-appearing RPE changes.

[b]ERG: (I) normal full field amplitudes; (II) normal scotopic but reduced photopic b wave amplitudes; (III) abnormal responses involving both rods and cones.

Table 1 reports the main demographic and clinical features of each enrolled patient and no significant differences emerged between the two groups as regards sex, age, disease onset, genotype and disease severity (Table 2).

No adverse events were reported during MP1-BF rehabilitation. Table 3 reports the main statistics of the selected features at baseline and follow-up time points. As summarized in Table 4, the treatment showed a positive effect on the visual function. Particularly, the patients undergoing training had a significant amelioration of reading abilities (Fig. 2); in particular, they were able to read smaller characters (i.e., decreased minimum print size) ($\beta = -0.77$ M-units, $P = 0.002$, $n = 24$) with a greater RS ($\beta = 16.91$ words/min, $P = 0.014$, $n = 24$) in comparison with the other group. BCVA significantly improved in patients in the TG compared with the CG (β –0.12 logarithm of the minumum angle of resolution [equivalent to 6 ETDRS letters], $P < .001$, $n = 24$). Furthermore, the mean sensitivity and fixation capability (FS2° and FS4°) improved significantly in patients who underwent rehabilitation ($\beta = 3.19$ dB, $P < .001$; $\beta = 17.93\%$, $P = 0.014$; and $\beta = 18.92\%$, $P = 0.002$ respectively; $n = 24$); the significant decrease of BCEA 68.2% ($\beta = -9.25°^2$, $P = 0.007$, $n = 24$), BCEA 95.4% (β –20.46°^{2}, $P = 0.007$, $n = 24$) and BCEA 99.6% (β –44.25°^{2}, $P = 0.008$, $n = 24$) confirmed the amelioration of fixation stability (Fig. 3).

Table 2. Baseline Clinical Data of Patient with STGD1 Stratified According to the Assigned Group

	TG	CG	*P* Value
Age (years)	29.6 ± 12.9	28.7 ± 11.3	0.85
Male	75.0	58.3	0.40
Age of onset (years)	20.1 ± 8.3	18.4 ± 7.5	0.61
Disease duration (years)	9.6 ± 6.6	10.3 ± 9.5	0.82
Fishman I/II/III	50.0/41.7/8.3	50.0/41.7/8.3	0.99
Lois I/II/III	66.7/25.0/8.3	66.7/16.7/16.7	0.78
Genotype: group A/B/C	75.0/16.7/8.3	66.7/25.0/8.3	0.76

Data are reported as mean ± standard deviation for continuous variables or frequency for categorical variables.

There were no significant changes in distance between the PRL and the fovea in degrees of visual angle; however, a significant decrease of DSS was found in the TG (β –1.57°, $P = 0.045$, $n = 24$) (Fig. 3). At the OCT examination, no significant changes in central retinal thickness and RPE-A were detected.

A comparison of the PVC activation in the retinotopic subdivisions PVC1-PVC4 are reported in Table 5, showing a significant effect of the TG versus CG ($P < 0.001$, $n = 19$). Moreover, we observed a statistically significant decrease of PVC activation over the follow-up in the CG, and a significant increase with age and female gender. The activation of left hemispheres did not differ statically from right ones. Similarly, no significant differences were observed between the stimulation of left eyes and right eyes.

Discussion

This is the first study in the literature to our knowledge in which the impact of visual rehabilitation on macular function was evaluated by analyzing PVC function in patients with STGD1, randomized to two groups (TG and CG) that did not show any statistically significant difference in the main visual and demographic parameters.

Some previous studies of structural and fMRI in nonhomogeneous groups of patients with macular degenerations, showed atrophy in the cerebral areas involved in visual function.[31,32] Moreover, they highlighted the persistence of activation of the primary visual area corresponding to the fovea when the PRL was stimulated in these patients.[33,34] Some authors linked the persistence of the activation of the cortical area corresponding with the fovea, after PRL stimulation, to a reorganization of the visual brain connections resulting from macular degeneration; in particular, this phenomenon was more frequently observed in patients with juvenile macular degeneration, when brain plasticity was more evident.[35] This theory is, however, much debated; in fact, other authors have shown that, in patients with late-onset macular degeneration, the persistent activation of foveal corresponding area was due to the activation of close areas (a top-down effect), especially in adults in whom less neuroplasticity phenomena could be expected.[36] To this regard, in our previous study[37] we showed stronger PVC activation in patients with STGD1 with a more preserved retinal function and macular structure, suggesting that the evaluation of neuronal reorganization could be performed only by considering retinal parameters, particularly ERG responses.

The main outcome of our study was to evaluate the effects of visual rehabilitation with MP1-BF on macular function and PVC activation. A previous work carried out by Vingolo et al.[11] evaluated the efficacy of rehabilitation with MP1-BF, in five patients with heterogeneous macular diseases (only one patient with STGD1), through 10 sessions of 10 minutes. At the end of the treatment the authors found a significant increase in the visual function parameters; however, the main limitations in that study were the patients with nonhomogeneous macular degeneration and the lack of a CG. A further study on a larger cohort of patients with STGD1 was performed by Verdina et al.,[38] who compared a group treated with MP1-BF and a CG. After eight treatment sessions that lasted 10 minutes each, a statistically significant improvement in fixation stability, BCVA, and RS was found in the treated group. Also in that study there were some limitations: the first is that the treatment was carried out only in one eye, and the second is that the small number of enrolled patients did not enable to perform a statistical analysis of predictive value on the specific clinical characteristics regarding the individual response to treatment.

In the current study, we analyzed a large group of patients with STGD1 treated with MP1-BF and compared with a CG of patients with STGD1; the

Table 3. Main Statistics of Selected Ophthalmologic Parameters at Baseline and Follow-up Time-Points for Each Group

	TG				CG			
	Baseline		Follow-up		Baseline		Follow-up	
	RE	LE	RE	LE	RE	LE	RE	LE
BCVA (logMAR)	0.71 ± 0.25	0.67 ± 0.32	0.64 ± 0.25	0.59 ± 0.28	0.78 ± 0.22	0.83 ± 0.18	0.82 ± 0.21	0.87 ± 0.15
	0.71 (0.65–0.85)	0.75 (0.62–0.85)	0.66 (0.59–0.77)	0.62 (0.57–0.79)	0.89 (0.72–0.92)	0.87 (0.79–0.95)	0.9 (0.76–0.97)	0.9 (0.83–1)
MPS (M)	2.04 ± 2.57	2.1 ± 2.65	1.5 ± 2.06	1.5 ± 2.07	1.89 ± 2	2.15 ± 2.64	1.97 ± 2	2.23 ± 2.63
	1.25 (0.8–2)	1.25 (0.8–1.63)	0.8 (0.8–1.06)	0.9 (0.75–1.06)	1.25 (0.95–2)	1.25 (0.8–2)	1.25 (1–2.13)	1.25 (0.95–2.13)
RS (words/min)	79.4 ± 31.2	77.8 ± 27.5	96.3 ± 34.1	96.7 ± 32.6	76.6 ± 27.9	76.7 ± 33.2	74.5 ± 27.5	77.5 ± 30.6
	76.2 (54–104.2)	81.5 (62.5–97)	99.8 (81–120)	99.2 (84.1–117)	81.5 (60.8–83.7)	80 (70–92.7)	77.7 (58.7–85.9)	80 (70.3–91)
MS (dB)	12.2 ± 5.1	12.7 ± 6.6	14 ± 5.9	14.6 ± 6.4	12 ± 6.4	11.9 ± 5.8	11.3 ± 6.9	11.4 ± 5.7
	12.8 (10.8–15.6)	14.7 (10.5–17.3)	15.3 (13.8–17.4)	16 (12.5–20)	13.1 (10–16.9)	13.1 (10.3–15.2)	13 (6.7–17.1)	12.3 (10–14)
FS 2° (%)	34.9 ± 25	35.5 ± 21.5	50.2 ± 23.8	47.3 ± 24.6	43.8 ± 19.1	43.8 ± 26.4	35.4 ± 22	36.2 ± 29.2
	31 (16.5–52.5)	33 (22.5–49)	40 (33.5–66.3)	45 (30–50)	39 (31–49.8)	33.5 (26.5–64.8)	35 (20.3–44.3)	36 (11.8–50)
FS 4° (%)	66 ± 30.3	70.8 ± 22.4	80.2 ± 14.1	82.2 ± 11.7	81 ± 13.5	76.3 ± 19.3	68.8 ± 22.9	66.1 ± 29.4
	75 (57.8–86.3)	78.5 (54–86)	80.5 (74.8–87.8)	84 (77.8–88.3)	83 (72.8–92.5)	75.5 (69.5–90.3)	76 (57.5–84)	79 (45–85.8)
BCEA 68.2% ($°^2$)	16.6 ± 18.9	16 ± 18	7.6 ± 4.3	7.1 ± 4.4	9.6 ± 10.9	8.7 ± 6.4	17.5 ± 19.4	11.1 ± 6.6
	9.7 (6.8–17.3)	12.3 (5.7–17.3)	8.6 (4.1–9.5)	6.3 (4.8–8.8)	6.7 (4.6–9.2)	7.7 (3.7–12)	8.5 (7.3–22.2)	10 (7.9–15.4)
BCEA 95.4% ($°^2$)	44.8 ± 50.8	43.1 ± 48.5	20.9 ± 11.8	19.4 ± 11.6	25.8 ± 29.4	23.5 ± 17.3	46.6 ± 52.3	30.6 ± 18.9
	26.1 (18.3–46.6)	33 (15.3–46.7)	23.2 (11–26.4)	17 (14.4–23.7)	18 (12.4–24.9)	20.8 (10–32.3)	21.4 (19.5–59.8)	27.1 (21.2–41.5)
BCEA 99.6% ($°^2$)	80.1 ± 90.8	76.9 ± 86.7	37.1 ± 20.9	34.4 ± 20.8	46.1 ± 52.5	42.1 ± 30.8	83.3 ± 93.2	53.7 ± 32.3
	46.6 (32.7–83.3)	59 (27.3–83.4)	41.5 (19.6–45.8)	30.4 (23.8–42.4)	32.2 (22.1–44.5)	37.2 (17.9–57.7)	37.9 (34.9–107)	48.4 (37.8–74.1)
PRL–E (°)	5.9 ± 3.7	5.2 ± 2.5	6.8 ± 4.2	6.1 ± 3.1	5 ± 3.5	5.4 ± 4.6	5.9 ± 3.5	6.4 ± 4.9
	4.5 (4–7)	4.5 (3–6.3)	5 (5–9)	6 (3.8–8)	4.5 (2–7)	3.5 (3–6.3)	5 (4–7)	5 (4.5–6.8)
PRL–A (°)	223 ± 122	160 ± 124	223 ± 114	191 ± 126	272 ± 78	137 ± 114	284 ± 81	135 ± 114
	258 (95–325)	115 (45–268)	255 (108–320)	193 (81–290)	293 (245–330)	100 (45–256)	325 (260–340)	90 (53–256)
DSS (°)	4.87 ± 5.64	4.12 ± 6.69	2.68 ± 5.77	3.52 ± 5.76	4.52 ± 6.96	4.62 ± 6.89	4.63 ± 6.61	4.42 ± 6.63
	3.75 (1.13–5.78)	0.9 (0.3–3.6)	0.15 (0–1.73)	0.75 (0.23–5.03)	0.9 (0.3–4.88)	0.9 (0.45–6.38)	1.05 (0.3–6.15)	1.2 (0.45–5.03)
CRT (µm)	122 ± 26	141 ± 45	128 ± 35	138 ± 46	142 ± 47	144 ± 44	133 ± 46	137 ± 41
	127 (98–145)	136 (120–146)	127 (100–147)	129 (110–147)	150 (120–180)	149 (126–169)	138 (114–157)	132 (125–161)
RPE-A (mm^2)	2.54 ± 4.77	2.33 ± 3.58	2 ± 3.27	2.35 ± 3.72	1.84 ± 2.96	2.69 ± 4.78	1.69 ± 2.08	2.65 ± 4.46
	0.8 (0.08–2.4)	0.7 (0.08–2.58)	0.7 (0–2.48)	0.35 (0.08–2.48)	0.9 (0–1.93)	0.8 (0.15–2.18)	1.15 (0.08–1.95)	0.8 (0.18–2.1)

Data are expressed as mean ± standard deviation; median (interquartile range). BCVA, best corrected visual acuity; BCEA, bivariate contour ellipse area; CRT, central retinal thickness; DSS, dense scotoma size; FS, fixation stability; LE, left eye; logMAR, logarithm of the minumum angle of resolution; MPS, minimum print size; MS, mean sensitivity; PRL-A, distance between the PRL and the fovea in a clockwise direction in retinal coordinates; PRL-E, distance between the PRL and the fovea in degrees of visual angle; RE, right eye; RPE-A, area of the RPE lesion; RS, reading speed.

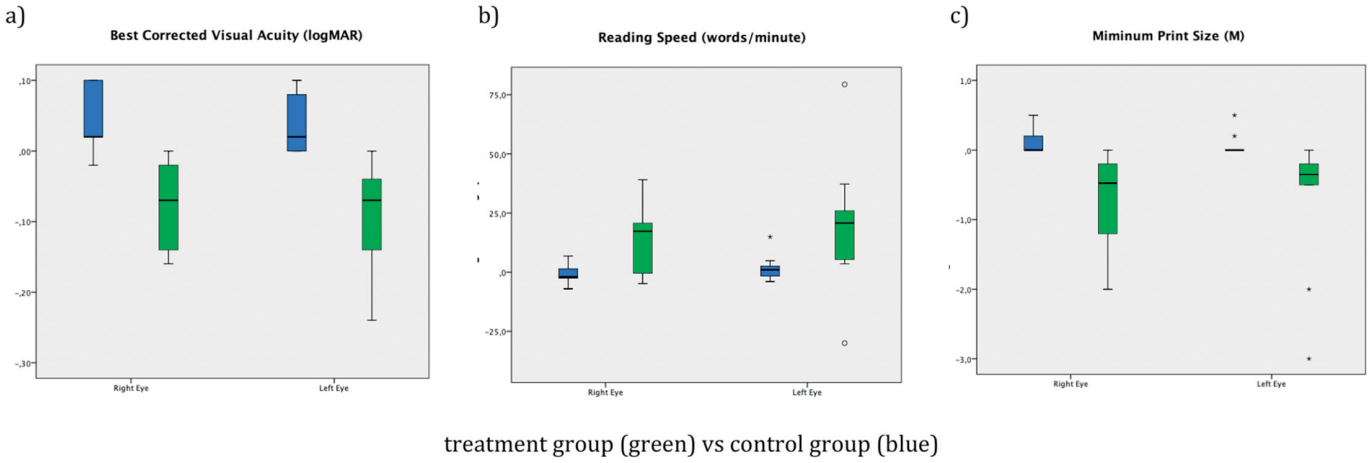

Figure 2. Change in visual reading test parameters: best corrected visual acuity (a), reading speed (b), minimum print size (c).

Table 4. Comparison of Change from Baseline of Selected Ophthalmologic Parameters in the Treatment Versus the Control Group

	Change from Baseline (TG vs. CG)		
	β	(95% CI)	*P* Value
BCVA (logMAR)	−0.12	(−0.17 to −0.08)	*<0.001*
MPS (M)	−0.77	(−1.27 to −0.28)	*0.002*
RS (words/min)	16.9	(3.4 to 30.4)	*0.014*
MS (dB)	3.2	(1.58 to 4.80)	*<0.001*
FS 2° (%)	17.93	(3.59 to 32.27)	*0.014*
FS 4° (%)	18.9	(7.0 to 30.9)	*0.002*
BCEA 68.2% (°^{2})	−9.25	(−16.01 to −2.48)	*0.007*
BCEA 95.4% (°^{2})	−20.5	(−37.51 to −3.40)	*0.007*
BCEA 99.6% (°^{2})	−44.3	(−66.8 to −11.7)	*0.008*
PRL-E (°)	0.14	(−1.91 to 2.19)	0.894
PRL-A (°)	11.5	(−66.7 to 89.6)	0.774
DSS (°)	−1.57	(−3.11 to −0.03)	*0.045*
CRT (µm)	11.59	(−3.7 to 26.9)	0.139
RPE-A (mm^2)	−0.19	(−1.00 to 0.63)	0.652

BCVA, best corrected visual acuity; BCEA, bivariate contour ellipse area; CI, confidence interval; CRT, central retinal thickness; DSS, dense scotoma size; FS, fixation stability; logMAR, logarithm of the minumum angle of resolution; MPS, minimum print size; MS, mean sensitivity; PRL-A, distance between the PRL and the fovea in a clockwise direction in retinal coordinates; PRL-E, distance between the PRL and the fovea in degrees of visual angle; RPE-A, area of the RPE lesion; RS, reading speed; in italics statistically significant *p*-value.

groups did not differ for sex, age, age of disease onset, or disease severity. Our data show that the treatment has a significant positive effect on visual function: reading capacities were improved, with a significant decrease of the print character size that the treated patients could read and a significant increase in the RS. In addition, a significant improvement in BCVA was assessed. Furthermore, a significant improvement in retinal sensitivity and fixation stability was noted in patients undergoing rehabilitation compared with the CG. In addition, although MP1 did not show significant changes in the eccentricity of the PRL after treatment, there was a significant reduction in the DSS; this finding can be explained by a better visual performance during MP1, but also by a more precise DSS assessment, owing to an improved stability of fixation that led to a decrease in the areas of absolute scotoma. Finally, we observed an increased activation of PVC in patients undergoing visual rehabilitation compared with CG. This finding is expected to be due to improvements in fixation stability related to the development of PRL, and particularly in the ability of fixate relatively small objects subtending 2°, such as letters in the word recognition task and fixation targets in both checkerboard and word recognition paradigms. These findings confirm that BF is an effective and noninvasive approach that improves residual visual function in patients with STGD1. Therefore, it could also be adopted in conjunction with other experimental strategies to optimize their effects on visual function, such as a selected area, nonatrophic and treated with gene therapy, could be trained as eccentric PRL by BF to maximize the improvement. Finally, these results suggest that biomarkers based on fMRI could be used as objective outcomes in STGD1 clinical trials for evaluation of visual function amelioration owing to experimental therapies.

The current study has some limits. First, the lack of control task in the CG did not enable to disregard the so-called placebo-expectancy effects, because subjects randomized to the TG have more expectations than those randomized to the CG. However, it is difficult to define a control task that could engender the

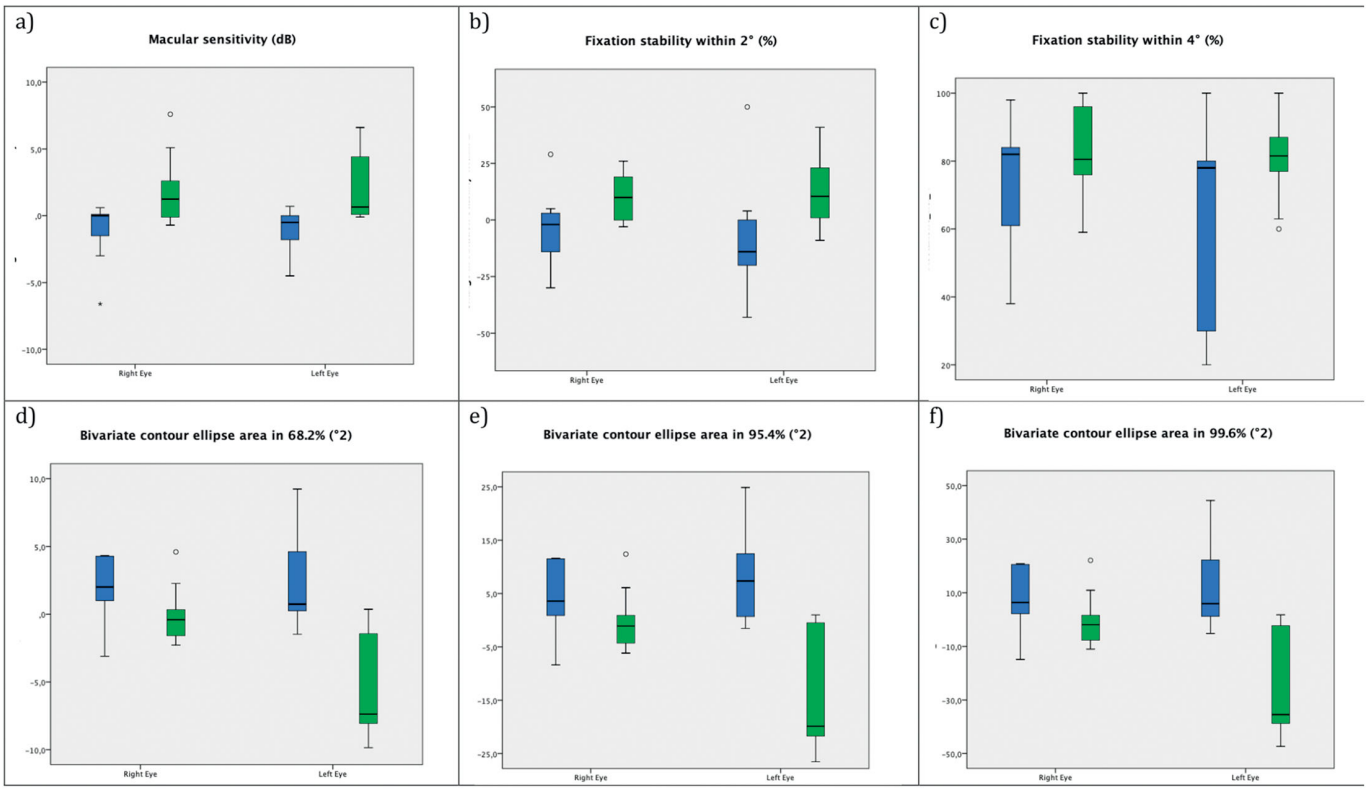

Figure 3. Changes in microperimetric parameters: macular sensitivity (a); fixation stability within 2° (b); fixation stability within 4° (c); bivariate contour ellipse area 68.2% (d); 95.4% (e); and 99.6% (f).

same expectations as the BF in the CG; in addition, the placebo-expectancy effects themselves have been considered as part of the usefulness of BF training.[39] Actually, all the previous studies on BF rehabilitation have no CG at all. Other limits are the small sample size and the short-term follow-up (3 months). For those reasons, future studies are needed to optimize the MP1-BF (e.g., number and schedule of sessions) and to

Table 5. Repeated-Measure Longitudinal Regression Model to Estimate Change in fMRI Activation in the Selected ROIs

			95% Confidence Interval		
Parameter	B	Standard Deviation	Inferior	Superior	*P* Value
CG	−1.221	0.1732	−1.56	−0.881	*<0.001*
TG (vs. CG)	0.56	0.0891	0.386	0.735	*<0.001*
PVC4 (vs. PVC1)	−0.119	0.1021	−0.319	0.081	0.243
PVC3 (vs. PVC1)	0.049	0.1107	−0.168	0.266	0.657
PVC2 (vs. PVC1)	−0.049	0.0932	−0.232	0.133	0.596
Age	0.02	0.0042	0.011	0.028	*<0.001*
Female	0.807	0.0957	0.619	0.995	*<0.001*
Left hemisphere	0.004	0.058	−0.109	0.118	0.939
Left eye	−0.077	0.1252	−0.322	0.168	0.539

The regression model shows a statistically significant decrease of PVC activation over the follow-up in the CG (first row); a significant effect of TG versus CG (second row) on PVC activation; a significant increase of PVC activation with age (sixth row) and female gender (seventh row). TG, treatment group; CG, control group; PVC, primary visual cortex; in italic significant *p*-value.

investigate the stability of its effect over time, particularly, in relationship with the decline of visual function owing to disease progression.

In conclusion, visual rehabilitation using MP1-BF has increased visual acuity and reading performances, probably because the stabilization of PRL contributes to the reactivation of brain areas involved in central vision. Therefore, rehabilitation with MP1-BF represents an effective, repeatable and noninvasive method that improves residual visual function in patients with STGD1.

Acknowledgments

Supported in part by the project "Image processing and development of novel algorithms to support diagnosis in ophthalmology" funded by Multidisciplinary Department of Medical, Surgical and Dental Sciences, University of Campania Luigi Vanvitelli (funds to PM).

Disclosure: **P. Melillo,** Sanofi R&D (R), Shire (R); **A. Prinster,** None; **V. Di Iorio,** Shire (R); **G. Olivo,** None; **F.M. D'Alterio,** None; **S. Cocozza,** Sanofi (R), Amicus (R); **M. Quarantelli,** None; **F. Testa,** Sanofi R&D (R), Shire (R); **A. Brunetti,** None; **F. Simonelli,** Sanofi R&D (R), Shire (R), Spark Therapeutics (R)

[*] PM, AP, AB and FS contributed equally to the work presented here and should therefore be regarded as equivalent authors.

References

1. Strauss RW, Ho A, Munoz B, et al. The Natural History of the Progression of Atrophy Secondary to Stargardt Disease (ProgStar) studies: design and baseline characteristics: ProgStar report no. 1. *Ophthalmology*. 2016;123:817–828.
2. Allikmets R, Singh N, Sun H, et al. A photoreceptor cell-specific ATP-binding transporter gene (ABCR) is mutated in recessive Stargardt macular dystrophy. *Nat Genet*. 1997;15:236–246.
3. Von Noorden GK, Mackensen G. Phenomenology of eccentric fixation. *Am J Ophthalmol*. 1962;53:642–660.
4. Whittaker SG, Budd J, Cummings RW. Eccentric fixation with macular scotoma. *Invest Ophthalmol Vis Sci*. 1988;29:268–278.
5. Fishman GA, Farber M, Patel BS, Derlacki DJ. Visual acuity loss in patients with Stargardt's macular dystrophy. *Ophthalmology*. 1987;94:809–814.
6. Noble KG, Carr RE. Stargardt's disease and fundus flavimaculatus. *Arch Ophthalmol*. 1979;97:1281–1285.
7. Rotenstreich Y, Fishman GA, Anderson RJ. Visual acuity loss and clinical observations in a large series of patients with Stargardt disease. *Ophthalmology*. 2003;110:1151–1158.
8. Kim LS, Fishman GA. Comparison of visual acuity loss in patients with different stages of Stargardt's disease. *Ophthalmology*. 2006;113:1748–1751.
9. Crossland MD, Culham LE, Kabanarou SA, Rubin GS. Preferred retinal locus development in patients with macular disease. *Ophthalmology*. 2005;112:1579–1585.
10. Scuderi G, Verboschi F, Domanico D, Spadea L. Fixation improvement through biofeedback rehabilitation in Stargardt disease. *Case Rep Med*. 2016;2016:4.
11. Vingolo EM, Salvatore S, Cavarretta S. Low-vision rehabilitation by means of MP-1 biofeedback examination in patients with different macular diseases: a pilot study. *Appl Psychophysiol Biofeedback*. 2009;34:127–133.
12. Andrade MA, Muro EM, Moran F. Simulation of plasticity in the adult visual cortex. *Biol Cybern*. 2001;84:445–451.
13. Altpeter E, Mackeben M, Trauzettel-Klosinski S. The importance of sustained attention for patients with maculopathies. *Vision Res*. 2000;40:1539–1547.
14. Buia C, Tiesinga P. Attentional modulation of firing rate and synchrony in a model cortical network. *J Comput Neurosci*. 2006;20:247–264.
15. Di Iorio V, Orrico A, Esposito G, et al. Association between genotype and disease progression in Italian Stargardt patients: a retrospective natural history study. *Retina*. 2019;39:1399–1409.
16. Fishman GA. Fundus flavimaculatus. A clinical classification. *Arch Ophthalmol*. 1976;94:2061–2067.
17. Sull AC, Vuong LN, Price LL, et al. Comparison of spectral/Fourier domain optical coherence tomography instruments for assessment of normal macular thickness. *Retina*. 2010;30:235–245.
18. Gregori G, Wang F, Rosenfeld PJ, et al. Spectral domain optical coherence tomography imaging of drusen in nonexudative age-related macular degeneration. *Ophthalmology*. 2011;118:1373–1379.
19. Melillo P, Testa F, Rossi S, et al. En face spectral-domain optical coherence tomography for the monitoring of lesion area progression in Stargardt disease. *Invest Ophthalmol Vis Sci*. 2016;57:OCT247–OCT252.

20. Fujii GY, de Juan E, Jr., Sunness J, Humayun MS, Pieramici DJ, Chang TS. Patient selection for macular translocation surgery using the scanning laser ophthalmoscope. *Ophthalmology*. 2002;109:1737–1744.
21. Chen FK, Patel PJ, Webster AR, Coffey PJ, Tufail A, Da Cruz L. Nidek MP1 is able to detect subtle decline in function in inherited and age-related atrophic macular disease with stable visual acuity. *Retina*. 2011;31:371–379.
22. McCulloch DL, Marmor MF, Brigell MG, et al. ISCEV Standard for full-field clinical electroretinography (2015 update). *Doc Ophthalmol*. 2015;130:1–12.
23. Lois N, Holder GE, Bunce C, Fitzke FW, Bird AC. Phenotypic subtypes of Stargardt macular dystrophy-fundus flavimaculatus. *Arch Ophthalmol*. 2001;119:359–369.
24. Ming J, Thulborn KR, Szlyk JP. Reproducibility of activation maps for longitudinal studies of visual function by functional magnetic resonance imaging. *Invest Ophthalmol Vis Sci*. 2012;53:6153–6163.
25. Friston KJ, Holmes AP, Poline JB, et al. Analysis of fMRI time-series revisited. *Neuroimage*. 1995;2:45–53.
26. Ashburner J, Friston K. Multimodal image coregistration and partitioning–a unified framework. *Neuroimage*. 1997;6:209–217.
27. Plank T, Frolo J, Brandl-Ruhle S, et al. Gray matter alterations in visual cortex of patients with loss of central vision due to hereditary retinal dystrophies. *Neuroimage*. 2011;56:1556–1565.
28. Wandell BA, Winawer J. Imaging retinotopic maps in the human brain. *Vision Res*. 2011;51:718–737.
29. Zeger SL, Liang K-Y, Albert PS. Models for longitudinal data: a generalized estimating equation approach. *Biometrics*. 1988;44:1049–1060.
30. Islam MA, Chowdhury RI. Generalized estimating equation. *Analysis of repeated measures data*. New York: Springer; 2017:161–167.
31. Olivo G, Melillo P, Cocozza S, et al. Cerebral involvement in stargardt's disease: a VBM and TBSS study. *Invest Ophthalmol Vis Sci*. 2015;56:7388–7397.
32. Hernowo AT, Prins D, Baseler HA, et al. Morphometric analyses of the visual pathways in macular degeneration. *Cortex*. 2014;56:99–110.
33. Masuda Y, Dumoulin SO, Nakadomari S, Wandell BA. V1 projection zone signals in human macular degeneration depend on task, not stimulus. *Cereb Cortex*. 2008;18:2483–2493.
34. Dilks DD, Baker CI, Peli E, Kanwisher N. Reorganization of visual processing in macular degeneration is not specific to the "preferred retinal locus". *J Neurosci*. 2009;29:2768–2773.
35. Baker CI, Peli E, Knouf N, Kanwisher NG. Reorganization of visual processing in macular degeneration. *J Neurosci*. 2005;25:614–618.
36. Baseler HA, Gouws A, Haak KV, et al. Large-scale remapping of visual cortex is absent in adult humans with macular degeneration. *Nat Neurosci*. 2011;14:649–655.
37. Melillo P, Prinster A, Di Iorio V, et al. Visual cortex activation in patients with Stargardt disease. *Invest Ophthalmol Vis Sci*. 2018;59:1503–1511.
38. Verdina T, Giacomelli G, Sodi A, et al. Biofeedback rehabilitation of eccentric fixation in patients with Stargardt disease. *Eur J Ophthalmol*. 2013;23:723–731.
39. Stroebel CF, Glueck BC. Biofeedback treatment in medicine and psychiatry: an ultimate placebo? *Semin Psychiatry*. 1973;5:379–393.